On the modelling of Coulomb friction

1999 J. Phys. A: Math. Gen. 32 2103

(http://iopscience.iop.org/0305-4470/32/11/006)

J. Phys. A: Math. Gen. **32** (1999) 2103–2113. Printed in the UK PII: S0305-4470(99)97599-6

On the modelling of Coulomb friction

S J Cull† and R W Tucker‡
Department of Physics, Lancaster University, Lancaster LA1 4YB, UK

Received 14 September 1998

Abstract. This paper analyses two different representations of Coulomb friction in the context of a dynamic simulation of the torsional vibrations of a driven drill-string. A simple model is used to compare the relative merits of a piecewise analytic approach using a discontinuous friction profile to a numerical integration using a smooth nonlinear representation of the Coulomb friction. In both cases the effects of viscous damping on the excitation of torsional relaxation oscillations are exhibited.

1. Introduction

When dealing with the dynamical evolution of a mechanical system in which frictional forces are active one is, in general, confronted with a particular type of nonlinear problem. The intermolecular interactions that give rise to sliding friction appear on a macroscopic level to act intermittently and the resulting forces generate a non-smooth temporal evolution. This type of force plays an important role in the generation of friction induced vibrations and is pivotal in the analysis of the stability of many mechanical systems. Despite its complex molecular origins the macroscopic description of sliding friction is now reasonably well understood over a vast range of phenomenology [4]. In the simplest situations the retarding force of 'kinetic' dry friction is sensibly constant as long as there is relative motion between the interacting surfaces. The subtlety, from a mathematical viewpoint, is that in the vicinity of zero relative motion the magnitude of Coulomb friction depends on the dynamic environment.

Systems that exhibit motion in which certain degrees of freedom are constant for an extended interval of time (ankylosis [5]) often contain forces (or torques) in their equations of motion that behave like Coulomb friction. One approach to the integration of such systems is to treat the problem in a piecewise manner in time. Each component of the piecewise solution relates to equations where the Coulomb friction-type forces are smooth functions of the motion. In such cases a prescription is required to connect the solutions corresponding to such distinct dynamical phases. If ankylosis occurs in a driven system a further prescription is required to determine the interval of time after which ankylosed degrees of freedom become unfrozen.

Various continuous approximations to the behaviour of Coulomb friction as a function of relative motion have been proposed in order to circumvent the need for such a piecewise analysis. Inevitably the threshold between 'static friction' and 'kinetic friction' behaviour is replaced by a smooth graph over the real line with at least two turning points as a function of the relative motion between the interacting surfaces. It is usually assumed that as long as the difference between the maximum static friction and the typical kinetic friction is not

† E-mail address: s.cull@lancaster.ac.uk
‡ E-mail address: r.tucker@lancaster.ac.uk

0305-4470/99/112103+11$19.50

excessive such continuous approximations yield acceptable phenomenological alternatives [2]. However, we are not aware of any detailed comparisons between dynamical evolutions based on these distinct approaches. It is therefore of interest to explore their relative merits in a simple model. In this article we integrate a simply driven, coupled two-degree of freedom model, subject to damping and Coulomb friction. This extends recent work [1] on the piecewise analysis of a single-degree of freedom system with friction.

A physically motivated prescription is given that enables a comparison to be made between a piecewise analytic solution in which the friction is non-analytic and a numerical simulation with a continuous and smooth Coulomb friction. In each case solutions to the equations of motion are sought that display both stable evolution to a steady state and friction induced relaxation oscillations. When the piecewise equations of motion are linear an analytic solution is available for a well defined interval of time. This offers a particular advantage over the numerical simulation with nonlinear smooth friction since it allows the dependence of the solution on the parameters in the system to be readily ascertained.

The model is motivated by the need to control torsional vibrations in the rotary components of an active drilling assembly such as that used in the exploration for oil or gas. An idealized system consists of an electric motor providing a source of external torque (the top-drive) connected via a vertical steel pipe (the drill-string) to a heavy rotating stabilizer and drill-bit (the bottom-hole assembly (BHA)). The equations of motion for the model arise naturally from the continuum mechanics of the drill-string with heavy attachments at each end [6, 7] if one neglects the finite time of propagation of torsional disturbances along the drill-string and replaces it with a simple torsional spring†. In [3] a continuous approximation to torque friction at the drill-bit was used to investigate the stability of friction-induced torsional relaxation vibrations in the model. The BHA is frictionally constrained due to the interaction of the drill-bit with the rock face while the top-drive is assumed to be free of friction but subject to a controlled torque designed to yield a steady rotary state. Parameter domains in the model where the system exhibits (torsional) relaxation oscillations are often referred to as regions of 'slip–stick' [8–12]. In a real oil-well drilling assembly active measures are imposed in attempts to avoid such configurations due to their destructive potential.

2. Equations of motion

Let $\alpha(t)$ and $\theta(t)$ represent the angular positions of the top-drive and the BHA at time t respectively. In terms of the approximation above their equations of motion are

$$J_T\ddot{\alpha}(t) + \mathcal{G}_m(t) + u(t) = 0 \tag{1}$$

$$J_B\ddot{\theta}(t) - u(t) + W\mathcal{F}(t) = 0 \tag{2}$$

where the parameters J_T and J_B are effective moments of inertia of the top-drive and BHA respectively and W denotes the average 'weight on bit' (WOB), assumed constant. The forcing function $\mathcal{G}_m(t)$ denotes the external torque delivered by the top-drive and is given by

$$\mathcal{G}_m(t) = \kappa_p(\dot{\alpha}(t) - \Omega_0) + \kappa_i(\alpha(t) - \Omega_0 t) \tag{3}$$

where κ_p and κ_i are the rotary speed control parameters and Ω_0 is the target angular speed. The function $u(t)$ describes the transmitted torque and damping due to viscous effects. It is given by

$$u(t) = k(\alpha(t) - \theta(t)) + \beta_v(\dot{\alpha}(t) - \dot{\theta}(t)) \tag{4}$$

† A torsional wave takes about a second to traverse the length of a 3000 m drill-string. This implies that one should model the torsional disturbances in the drill-string by a wave equation. The influence of such a retardation on the dynamical evolution of torsional distrurbances induced by friction can be found in [7]. The effects therein justify the simplification in ignoring the continuum nature of the drill-string to a first approximation.

where $k > 0$ is the 'spring constant' of the drill-string regarded as a torsional spring and $\beta_v > 0$ is a viscous damping constant. The friction profile $\mathcal{F}(t)$ models the dependence of the friction torque on the relative motion between the BHA and the rock surface. It is assumed throughout, that the drill-bit is in contact with the rock surface. In the context of the model under discussion the approach based on a piecewise construction of the solution uses a friction profile given by

$$\mathcal{F}(t) = \begin{cases} C_f \operatorname{sgn}(\dot\theta(t)) & & \dot\theta(t) \neq 0 \\ \begin{cases} \dfrac{1}{W}u(t) & |u(t)| \leqslant WS_f \\ S_f \operatorname{sgn}(u(t)) & \text{otherwise} \end{cases} & & \dot\theta(t) = 0. \end{cases} \tag{5}$$

The constant C_f describes the kinetic friction component and S_f the static friction component. Both C_f and S_f are positive constants with $S_f > C_f$. As examples of continuous approximations to this profile one may cite [2, 3, 13]. For the approach based on a continuous friction profile we compare the effects of (5) with the three-parameter representation

$$\mathcal{F}(t) = \beta\left(\tanh(\dot\theta(t)) + \frac{A\dot\theta(t)}{1 + B\dot\theta(t)^2}\right) \tag{6}$$

where $-\infty \leqslant \dot\theta \leqslant \infty$ and the constants f_t, γ, β, A, and B are all positive.

3. Motion with discontinuous friction

The analysis of (1) and (2) using (5) is facilitated by introducing the domains $\mathrm{SLP}_\pm$ and STK defined by:

$$\mathrm{SLP}_+ = \{(\alpha, \dot\alpha, \theta, \dot\theta) | \dot\theta > 0\} \tag{7}$$

$$\mathrm{SLP}_- = \{(\alpha, \dot\alpha, \theta, \dot\theta) | \dot\theta < 0\} \tag{8}$$

$$\mathrm{STK} = \{(\alpha, \dot\alpha, \theta, \dot\theta) | \dot\theta = 0\}. \tag{9}$$

In each domain, (5) is either constant or equal to $\frac{1}{W}u(t)$ as shown in table 1. In general the system passes from the domain $\mathrm{SLP}_\pm$ to $\mathrm{SLP}_\mp$ via STK. If the system experiences ankylosis due to $\theta(t)$ being constant for a non-zero interval of time then the system resides in STK during that interval. System motion in $\mathrm{SLP}_\pm$ describes 'bit-slip' while system motion with ankylosis in STK describes 'bit-stick'. Henceforth we refer simply to 'slip' and 'stick' and call the motion of θ in SLP_+ an *upstroke* and the motion of θ in SLP_- a *downstroke*.

3.1. Transition conditions

In order to join the piecewise solutions to equations (1) and (2) one must specify conditions that relate the motions in different domains. Let $t = t_a$ be the time at which $\dot\theta$ vanishes. Then a condition is required to determine whether the motion proceeds smoothly in time or is arrested

Table 1. The value of $\mathcal{F}(t)$ in the three domains.

Domain	Friction	
SLP_+	$\mathcal{F}(t) = C_f$	
SLP_-	$\mathcal{F}(t) = -C_f$	
STK	$\mathcal{F}(t) = \begin{cases} \dfrac{1}{W}u(t) & |u(t)| \leqslant WS_f \\ S_f \operatorname{sgn}(u(t)) & \text{otherwise.} \end{cases}$	

by friction. If the latter occurs another condition is required to determine the time $t = t_b$ at which the transition from 'stick' to 'slip' occurs. The conditions for transitions between the different domains are given in terms of t_a and t_b. In the model under discussion only θ is prone to ankylosis although the generalization to more complicated systems in which several degrees of freedom may become frozen at different times is immediate. We also assume here that the dynamic magnitude of the top-torque is unconstrained although in practice this would be limited by the stalling characteristics of the drive motor.

3.1.1. $SLP_{\pm} \rightarrow SLP_{\mp}$. The equations of motion for an upstroke or a downstroke are given by

$$J_T\ddot{\alpha} + \kappa_p(\dot{\alpha} - \Omega_0) + \kappa_i(\alpha - \Omega_0 t) + u = 0 \tag{10}$$

$$J_B\ddot{\theta} - u + WC_f \operatorname{sgn}[\dot{\theta}] = 0. \tag{11}$$

The time t_a, at which an upstroke or a downstroke ends, is found by solving

$$\dot{\theta}(t_a) = 0$$

for the root nearest to, but greater than, the time at which that particular stroke started. If t_a exists, the condition for an upstroke to be followed by a downstroke or vice versa at $t = t_a$ is

$$|u(t_a)| > WC_f. \tag{12}$$

3.1.2. $SLP_{\pm} \rightarrow STK$ with ankylosis. If the condition (12) is violated then, stick will occur starting at t_a. Thus the condition for a transition from 'slip' to 'stick' to occur at t_a is

$$|u(t_a)| \leqslant WC_f. \tag{13}$$

3.1.3. $STK \rightarrow SLP_{\pm}$. If the transition from 'slip' to 'stick' occurs at time t_a, then during 'stick'

$$\theta(t) = \theta(t_a) \tag{14}$$

is constant. However, α will continue to evolve. While θ is frozen the equation of motion (1) for α becomes:

$$J_T\ddot{\alpha}(t) + \kappa_p(\dot{\alpha}(t) - \Omega_0) + \kappa_i(\alpha(t) - \Omega_0 t) + k(\alpha(t) - \theta(t_a)) + \beta_v(\dot{\alpha}(t)) = 0 \tag{15}$$

with initial conditions fixed by the values of α and $\dot{\alpha}$ at $t = t_a$. This equation is readily solved solve for $\alpha(t)$. The evolution may increase the transmitted torque sufficiently to unfreeze θ. We assume that the θ coordinate will remain frozen until the transmitted torque is large enough to overcome the static friction at some time $t_b > t_a$. i.e. when

$$u(t_b) = WS_f. \tag{16}$$

Thus the transition from 'stick' to 'slip' will occur at some time t_b given by the root of

$$u(t_b) \equiv k(\alpha(t_b) - \theta(t_a)) + \beta_v(\dot{\alpha}(t_b)) = WS_f \tag{17}$$

nearest to but greater than t_a. If time t_b does not exist then the system will remain in 'stick'.

3.2. Piecewise constructed solutions

The equations (1) and (2) with (3) may be solved analytically in those domains where the friction profile (5) is constant. In domains where the BHA is in a slip phase the general solution takes the form

$$\begin{pmatrix} \alpha(t) \\ \theta(t) \end{pmatrix} = \sum_{r=1}^{4} c_r \boldsymbol{k}_0(\lambda_r) \mathrm{e}^{\lambda_r t} + \boldsymbol{e}t + \boldsymbol{d} \tag{18}$$

where the λ_r are given by the roots of $\det(f(\lambda)) = 0$ for

$$f(\lambda) = \begin{pmatrix} J_T\lambda^2 + (\kappa_p + \beta_v)\lambda + (\kappa_i + k) & -\beta_v\lambda - k \\ -\beta_v\lambda - k & J_B\lambda^2 + \beta_v\lambda + k \end{pmatrix}. \tag{19}$$

The parameters are chosen so that the roots are distinct. The eigenvectors $\boldsymbol{k}_0(\lambda_r)$ associated with λ_r are given by

$$f(\lambda_r)\boldsymbol{k}_0(\lambda_r) = 0 \tag{20}$$

and the vectors $\boldsymbol{d}$ and $\boldsymbol{e}$ are defined by

$$\boldsymbol{d} = \begin{pmatrix} \frac{1}{\kappa_i} \\ \frac{1}{\kappa_i} + \frac{1}{k} \end{pmatrix} WC_f \operatorname{sgn}(\dot{\theta}) \tag{21}$$

$$\boldsymbol{e} = \begin{pmatrix} \Omega_0 \\ \Omega_0 \end{pmatrix} \tag{22}$$

for some target speed Ω_0. The constants c_r are determined by the configuration at the start of a particular slip phase.

In a domain where the BHA is in a stick phase with $t > t_a$ the general solution takes the form

$$\alpha(t) = C_1\mathrm{e}^{-\frac{1}{2}\lambda_+ t} + C_2\mathrm{e}^{-\frac{1}{2}\lambda_- t} + h(t) \tag{23}$$

$$\theta(t) = \theta(t_a) \tag{24}$$

where $\lambda_\pm$ (assumed distinct) are given by

$$\lambda_\pm = \frac{\kappa_p + \beta_v \pm \sqrt{(\kappa_p + \beta_v)^2 - 4J_T(\kappa_i + k)}}{J_T} \tag{25}$$

and

$$h(t) = \frac{k^2\theta(t_a) + \kappa_i k\theta(t_a) + \kappa_p k\Omega_0 - \kappa_i\Omega_0\beta_v + (\kappa_i k\Omega_0 + \kappa_i^2\Omega_0)t}{(\kappa_i + k)^2}. \tag{26}$$

The constants C_1 and C_2 are determined by the configuration at the start of the interval of stick.

If the initial conditions at $t = \tau$ are $\alpha(\tau) = \alpha_\tau$, $\dot{\alpha}(\tau) = \dot{\alpha}_\tau$, $\theta(\tau) = \theta_\tau$, $\dot{\theta}(\tau) = \dot{\theta}_\tau$ and $\dot{\theta}_\tau \neq 0$ then the motion starts off in slip. If there exists a time $t_a > \tau$ for which $\theta(t_a) = 0$, then at this time, the motion will either carry on in slip or a transition to stick will occur. To determine the evolution, the transition rules are used. If $\dot{\theta}_\tau = 0$ then the motion will start off in slip if $u(\tau) > WS_f$, otherwise the system starts off in stick, and stays in this state for an interval $t_b - \tau$ where the time $t_b > \tau$ is calculated using equation (17). Since α and θ are continuous functions of time, at each transition the end conditions for the previous piece of the solution form the initial conditions for the subsequent segment of evolution thereby determining the nature of the solution.

Table 2. Canonical values of the parameters in MKS units.

J_B	446 kg m^2
k	315 kg m^2 s^{-2}
W	1×10^5 kg m s^{-2}
Ω_0	13.09 rad s^{-1}
κ_p	750 kg m^2 s^{-1}
κ_i	50 kg m^2 s^{-2}
β_v	0 kg m^2 s^{-1}
C_f	0.041 m
S_f	0.100 m
β	$\frac{1}{27}$ m
A	20
B	20

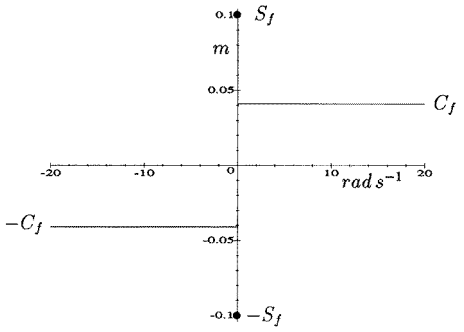

Figure 1. The piecewise Coulomb friction profile.

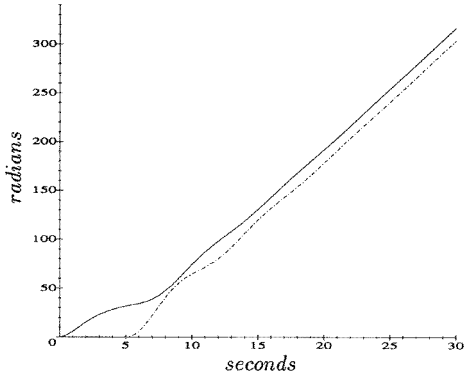

Figure 2. Piecewise constructed solutions for $\alpha(t)$ (full curve), $\theta(t)$ (chain curve).

4. Results

4.1. Piecewise solutions with zero viscous damping

In terms of the above analytic forms and the transition rules one may explore the dependence of the initial conditions in determining piecewise synthesized solutions. In this section damping effects are ignored and unless otherwise stated the results are calculated using the canonical values of the parameters shown in table 2. A plot of the piecewise defined Coulomb friction profile using these parameters is shown in figure 1.

Figure 2 is a plot of the angular position of the top-drive and BHA (chain curve) as a function of time. The corresponding angular velocities are shown in figure 3. In this solution the system exhibits transient torsional oscillations, both the top-drive and BHA evolving towards a stationary target rotary speed Ω_0. The initial conditions are chosen so that initially the drill-bit is stuck. After $t \approx 5$ s the transmitted torque, $u(t)$, is enough to overcome the static friction at the BHA. In contrast figures 4 and 5 depict a solution in which torsional relaxation oscillations are excited. The angular velocities of the top-drive and BHA do not tend towards the target speed and the BHA repeatedly slips and sticks.

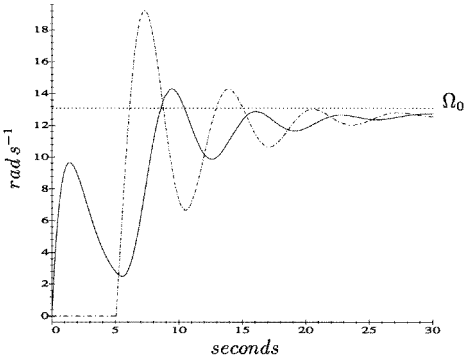

Figure 3. Piecewise constructed solutions for $\dot{\alpha}(t)$ (full curve), $\dot{\theta}(t)$ (chain curve).

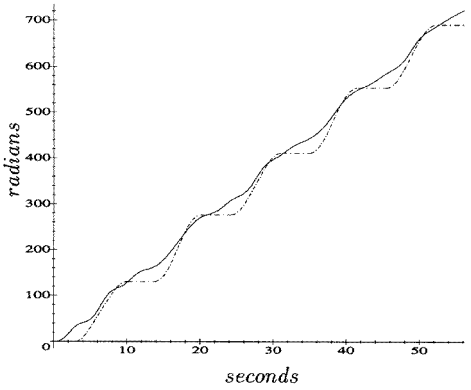

Figure 4. Piecewise constructed solutions for $\alpha(t)$ (full curve), $\theta(t)$ (chain curve), with $\kappa_p = 50$ kg m^2 s^{-1}, $\kappa_i = 750$ kg m^2 s^{-2} and other parameters taking the canonical values.

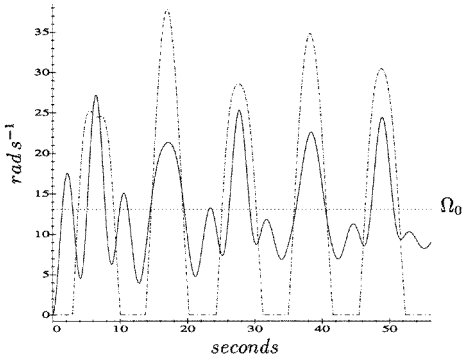

Figure 5. Piecewise constructed solutions for $\dot{\alpha}(t)$ (full curve), $\dot{\theta}(t)$ (chain curve), with $\kappa_p = 50$ kg m^2 s^{-1}, $\kappa_i = 750$ kg m^2 s^{-2} and other parameters taking the canonical values.

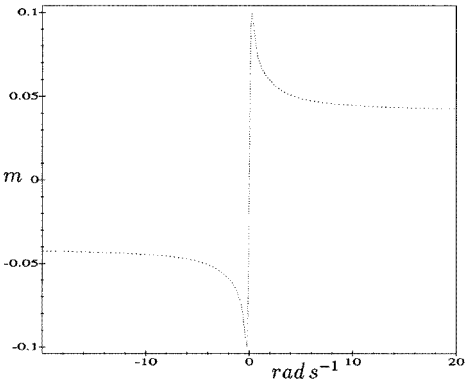

Figure 6. The Continuous simulation profile for Coulomb friction.

4.2. Comparison of solutions to those with zero viscous damping and continuous friction

The piecewise solutions above may be contrasted with those calculated using the continuous nonlinear friction profile (6). This friction profile is plotted in figure 6 and compared with the piecewise friction profile in figure 7. The value $|S_f|$ of the static friction in the piecewise friction profile occurs at the turning points in the continuous friction profile and the latter tends towards $|C_f|$ for large values of angular speed.

The solutions of the equations of motion (1)–(4) (with zero viscous damping), and (6) are obtained by numerical integration from a set of initial conditions. The solutions corresponding to a steady evolution of α and θ to their target values are displayed in figure 9 together with the corresponding solutions synthesized by the piecewise approach for comparison. A similar comparison for the corresponding angular speeds is made in figure 10. By changing the control parameters κ_p and κ_i the system exhibits torsional relaxation oscillations induced by the continuous friction profile (6). The resulting solutions are compared with the previous piecewise solutions in figures 11 and 12. (The key in figure 8 shows the representation of each

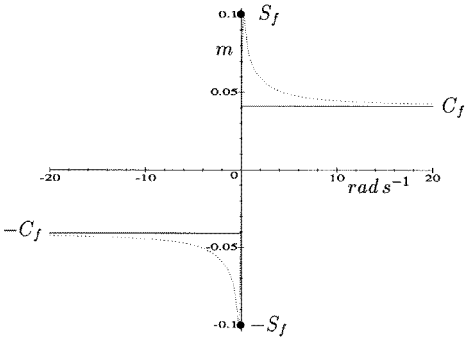

Figure 7. Comparison of the continuous nonlinear friction profile with the piecewise linear one.

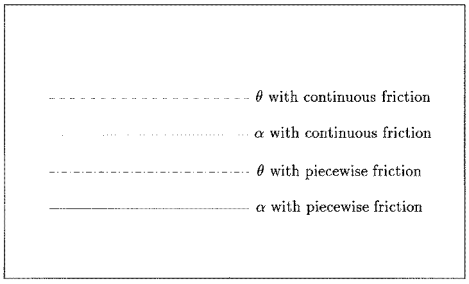

Figure 8. A key to the linestyles used in the following comparisons (figures 9–12).

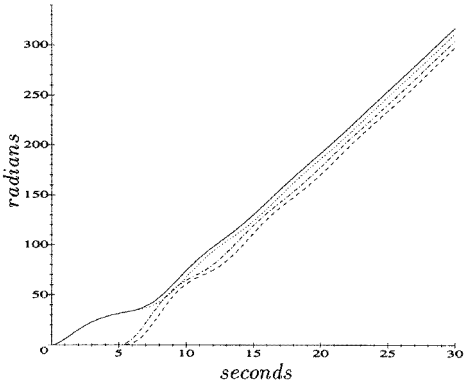

Figure 9. Comparison of $\alpha(t)$ and $\theta(t)$ generated with piecewise and continuous friction profiles.

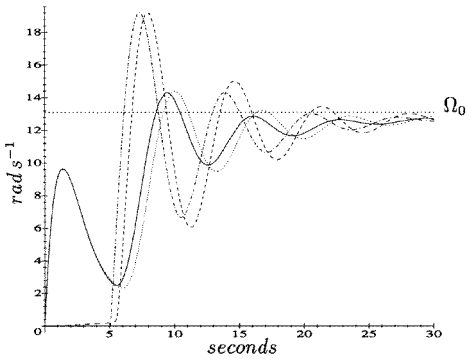

Figure 10. Comparison of $\dot{\alpha}(t)$ and $\dot{\theta}(t)$ generated with piecewise and continuous friction profiles.

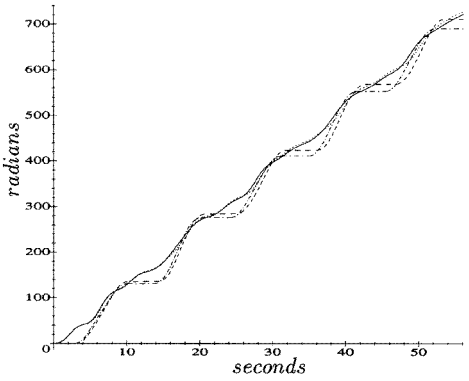

Figure 11. Comparison of $\alpha(t)$ and $\theta(t)$ generated with piecewise and continuous friction profiles, $\kappa_p = 50\ \mathrm{kg\ m^2\ s^{-1}}$, $\kappa_i = 750\ \mathrm{kg\ m^2\ s^{-2}}$, and other parameters taking the canonical values.

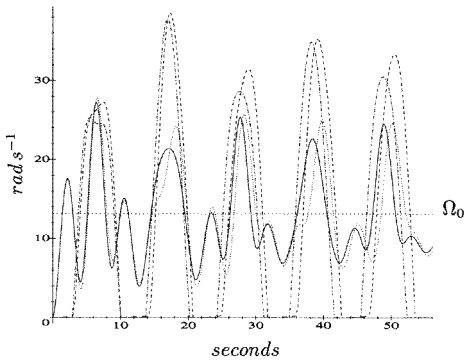

Figure 12. Comparison of $\dot{\alpha}(t)$ and $\dot{\theta}(t)$ generated with piecewise and continuous friction profiles, $\kappa_p = 50\ \mathrm{kg\ m^2\ s^{-1}}$, $\kappa_i = 750\ \mathrm{kg\ m^2\ s^{-2}}$, and other parameters taking the canonical values.

linestyle in the comparison plots.) These comparisons indicate that for the initial condition under consideration both the piecewise-analytic (5) and continuous friction (6) approach yield

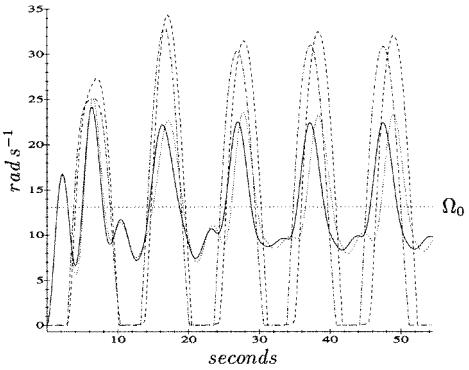

Figure 13. The effect of viscous damping on $\dot{\alpha}(t)$ and $\theta(t)$ with $\beta_v = 50$ kg m^2 s^{-1}, $\kappa_p = 50$ kg m^2 s^{-1}, $\kappa_i = 750$ kg m^2 s^{-2} and other parameters taking the canonical values. The effect of viscous damping is similar in both the piecewise constructed solution and the solution generated from the continuous friction profile.

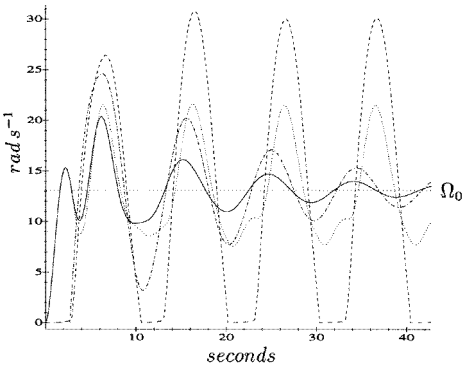

Figure 14. The effect of viscous damping on $\dot{\alpha}(t)$ and $\theta(t)$ with $\beta_v = 150$ kg m^2 s^{-1}, $\kappa_p = 50$ kg m^2 s^{-1}, $\kappa_i = 750$ kg m^2 s^{-2} and other parameters taking the canonical values. The viscous damping inhibits the formation of torsional relaxation oscillations in the piecewise constructed solution, although it persists in the solution generated from the continuous friction profile.

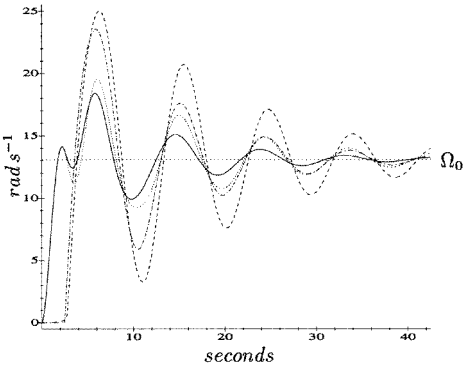

Figure 15. The effect of viscous damping on $\dot{\alpha}(t)$ and $\theta(t)$ with $\beta_v = 250$ kg m^2 s^{-1}, $\kappa_p = 50$ kg m^2 s^{-1}, $\kappa_i = 750$ kg m^2 s^{-2} and other parameters taking the canonical values. The large viscous damping inhibits the formation of torsional relaxation oscillations in both types of solution.

acceptable alternatives when modelling the equations of motion (1)–(4) in the absence of viscous damping. Further simulations indicate that deviations in the two approaches begin to arise when the the ratio $C_f/S_f < 0.2$, the other parameters being held fixed. According to [1], few mechanical system experience this type of Coulomb friction.

5. The effect of viscous damping

To explore the effects of viscous damping in the model the previous computations have been repeated with $\beta_v \neq 0$. Figures 13–15 display the effect of increasing the viscous damping parameter β_v. The other parameters are chosen such that slip–stick oscillations are excited when $\beta_v = 0$. Figure 13 shows the effect of $\beta_v = 50$ kg m^2 s^{-1} on the slip–stick solution shown in figure 12. The solutions corresponding to piecewise and continuous friction profiles compare well and it can be observed that the effect of the viscous damping is to slightly reduce the duration of BHA stick. Figure 14 shows the effect with $\beta_v = 150$ kg m^2 s^{-1}. The two kinds of solutions are now visibly different. The solution synthesized in a piecewise manner shows that viscous damping of this magnitude eliminates the relaxation oscillations and the system exhibits damped torsional oscillations. The solution generated by numerical analysis

with the continuous friction profile shows a larger reduction in the stick intervals compared to those in figure 13. Finally in figure 15 with $\beta_v = 250$ kg m^2 s^{-1} both types of simulation exhibit damped torsional oscillations.

6. Conclusions

The model in section 2 has been explored using two different approaches based on different ways of simulating Coulomb friction. It has been observed that for certain values of the parameters in the equations of motion and in the absence of viscous damping the use of the piecewise approach to the integration using the piecewise linear friction profile (5) yields a solution that is well approximated by that obtained from numerical integration using the smooth nonlinear friction profile (6). The agreement between the two simulations begins to break down as the magnitude of the static friction torque departs from the kinetic one in (5). An increase in viscous damping in the system has a similar effect. Furthermore it is found that large viscous damping inhibits the formation of torsional relaxation oscillations.

A particular advantage of the piecewise approach is that the integration can be performed analytically, thereby enhancing the speed of the simulation. The analytic form of the solution in each phase also enables one to gauge the importance of various parameters on the evolution of the system. For example, for small viscous damping the transition from slip to stick is less likely to occur for small values of the W (see equation (13)) and repeated slip–stick is thereby less likely to occur. Similarly the duration of the stick period, if it occurs, will be shorter (see equation (16)) for smaller values of W. Repeated sticking and slipping is also less likely for higher values of Ω_0.

A potential drawback associated with this method is the time required to calculate the extent of each segment of the evolution. Thus if a slip interval starts at $t = t_s$ and ends at $t = t_{s+1}$ then t_{s+1} is given from (18) by the root of $\dot{\theta}(t_{s+1}) = 0$ nearest to but greater than t_s. In this case the constants c_r are determined by $\alpha(t_s)$, $\theta(t_s)$, $\dot{\alpha}(t_s)$ and $\dot{\theta}(t_s)$. Considerable computational time may be required to locate the appropriate root in situations where the roots become dense. This is perhaps the main reason why the continuous approximations to Coulomb friction are used in numerical simulations. Of course if the equations at the outset are not amenable to piecewise linear integration it may be the only alternative. The conclusion here is that modulo the caveats concerning the relative size of static and kinetic components of the friction and the strength of viscous damping in the system the simulations using the continuous approximation (6) to Coulomb friction in the equations of section 2 are effective.

Acknowledgments

We are most grateful to F Abbassian, M Fear and S Parfitt for their valuable advice in this investigation and to the Leverhulme Trust, EPSRC and BPX for financial support.

References

[1] B Armstrong and B Amin 1996 PID control in the presence of static friction: a comparison of algebraic and describing function analysis *Automatica* **32** 679–92

[2] M T Bengisu and A Akay 1991 *Interaction and Stability of Friction and Vibrations, Fundamentals of Friction: Macroscopic and Microscopic Processes (NATO ASI Series E: Applied Sciences 220)* (Dordrecht: Kluwer) pp 553–66

[3] V A Dunayevsky and F Abbassian 1995 Application of stability approach to bit dynamics *Proc. SPIE* SPE 30478

[4] F J Elmer 1997 Non-linear dynamics of dry friction *J. Phys. A: Math. Gen.* **30** 6057–63

[5] R A Frazer 1938 *Elementary Matrices* (Cambridge: Cambridge University Press) pp 332–57

[6] R W Tucker and C Wang 1999 On the effective control of torsional vibrations in drill-string dynamics *J. Sound Vib.* to appear
[7] R W Tucker and C Wang 1999 An integrated model for drill string dynamics *J. Sound Vib.* to appear
[8] Seon-Woo Lee and Jong-Hwan Kim 1995 Robust adaptive stick–slip friction compensation *IEEE Trans. Ind. Electron.* **42** 474–9
[9] B Armstrong 1993 Stick slip and control in low-speed motion *IEEE Trans. Autom. Control* **38** 1483–96
[10] P E Dupont 1994 Avoiding stick–slip through PD control *IEEE Trans. Autom. Control* **39** 1094–7
[11] S C Southward, C J Radcliffe and C R MacCluer 1991 Robust nonlinear stick–slip friction compensation, *J. Dyn. Syst. Meas. Control* **113** 639–45
[12] Chi-Thuan Cao 1993 Fuzzy compensator for stick–slip friction *Mechatronics* **3** 783–94
[13] R W Tucker and C Wang 1997 The excitation and control of torsional slip–stick in the presence of axial-vibrations *BP Report* http://www.lancs.ac.uk/users/SPC/research/theory/bp/slip.pdf